Agricultural and Forest Meteorology 300 (2021) 108325

Contents lists available at ScienceDirect

Agricultural and Forest Meteorology

journal homepage: www.elsevier.com/locate/agrformet

Impacts of deep-rooted fruit trees on recharge of deep soil water using stable and radioactive isotopes

Peijun Shi [a], Yannan Huang [a], Wangjia Ji [a], Wei Xiang [a], Jaivime Evaristo [a,b], Zhi Li [a,*]

[a] State Key Laboratory of Soil Erosion and Dryland Farming on the Loess Plateau, College of Natural Resources and Environment, Northwest A&F University, Yangling, 712100, China
[b] Copernicus Institute of Sustainable Development, Utrecht University, Utrecht, Netherlands

ARTICLE INFO

Keywords:
Water isotopes
Recharge mechanism
Subsurface water reservoir
Loess Plateau
Land use change

ABSTRACT

Deep-rooted fruit trees mine more water from deep soils than their shallow-rooted counterparts. Understanding how deep soil water (DSW) is replenished and subsequently depleted by deep-rooted fruit trees, therefore, are important for informing sustainable water resources management particularly in arid regions. In this study, we collected soil samples from the surface down to 20 m under four land use types (farmland, 8-year apple orchard, 12-year peach orchard, and 25-year apple orchard) in China's Loess Plateau. We then measured the soil water content, stable (δ^2H and $\delta^{18}O$) and radioactive (^3H) isotopic compositions. The radioactive isotope was used to constrain the age of soil water while the stable isotopes were used to determine the types of storms that would have contributed to recharging the DSW. We then implemented a soil water balance model to identify the mechanisms underlying the changes in DSW. Mechanistically, our results show that water movement in these soils was predominantly via piston flow. The age of DSW below 8 m was determined to be older than 55 years. Altogether, these results support an interpretation that DSW may have only been recharged by high-intensity, low-frequency rainfall events during the wet season (July to September), but that the magnitude of DSW recharge was likely to be influenced by subsequent water mining by deep-rooted fruit trees. The deep-rooted fruit trees consumed more DSW than farmland vegetation, substantially limiting the magnitude of DSW recharge under the orchards. Our simple soil water balance model, informed by water stable isotopes and supplemented with information from tritium, provides a technique for partitioning soil water balance (SWB) and insights into the long-term effects of land use change on water resources in arid regions.

1. Introduction

The sustainability of soil water resources underpins food security and ecosystem function (Bryan et al., 2018; Chen et al., 2015; Wang et al., 2018). Despite the fundamental importance of soil water, however, what determines the sustainability of this resource in space and time remains poorly understood (Blöschl et al., 2019; Tang, 2019). Whereas climate exerts the most important control on spatiotemporal variability of soil water storage in the long-term and at larger scales (Li et al., 2010; Oki and Kana, 2006), vegetation is the most important controls in the short-term and at regional scales (Chen et al., 2007; Geris et al., 2015; Wang et al., 2011). Thus, land cover and land use change, in a large part because of human activities, can lead to changes in soil water reservoirs (Deng et al., 2020; Schwarzel et al., 2019). Nowhere is the interaction between land cover and soil water more pronounced than in semi-arid and arid regions (Cao et al., 2018; Carrière et al., 2020; Wang et al., 2011). In these regions, deep-rooted vegetation, mostly trees, may deplete deep-soil water (DSW) (Jia et al., 2017; Jian et al., 2015; Mendham et al., 2011; Wang et al., 2020; Zhang et al., 2018), which in turn negatively impacts on vegetation productivity and survival. It is therefore important to understand how DSW under deep-rooted vegetation in these regions is replenished.

To control the soil erosion, the land use / cover pattern has been substantially changed in the Loess Plateau of China since the 1990s (Li et al., 2016; Peng and Li, 2018). An important land use change type is afforestation on native cropland and grassland with areas up to 1.0×10^5 km^2 by 2020 (Du et al., 2020), which has been reported to result in severe soil water deficit (1037−1531 mm) in deep soil layers (Huang and Shao, 2019). Among forestlands, the deep-rooted fruit trees have been largely planted to increase economic benefit (about 7252 km^2) (Jia

* Corresponding author.
E-mail address: lizhibox@nwafu.edu.cn (Z. Li).

https://doi.org/10.1016/j.agrformet.2021.108325
Received 6 December 2020; Accepted 10 January 2021
Available online 23 January 2021

et al., 2014; Peng et al., 2017); however, our previous studies showed that the tradeoff between economic benefit and subsurface water sustainability is a big issue (Huang et al., 2018; Li et al., 2019a). In consequence, the possibility of soil water being recharged under the deep-rooted fruit trees should be explored for sustainable management of water resources and agriculture.

Monitoring the dynamics of soil water is helpful in determining the possibility of recharge, but it needs long-term observation to provide enough information (Kendy et al., 2003; Scanlon et al., 1997). Conversely, tracer method is superior to analysis of water movement in arid regions, among which water isotopes (^{2}H, ^{18}O and ^{3}H) have been widely used to explore the sources (Brooks et al., 2009; Li et al., 2019b, 2017b), pathways (Allison and Hughes, 1983; Li et al., 2017a; Zimmermann et al., 1966), and ages of water (Sprenger et al., 2019). The stable isotopes (^{2}H, ^{18}O) are more proper to identify sources of young water (a few years) and estimate the soil evaporation loss (Allen et al., 2019; Evaristo et al., 2019; Sprenger et al., 2017), while the radioactive isotope (^{3}H) is superior to determine ages of water with decades and quantify deep drainage (Lin and Wei, 2006; Zhang et al., 2017). The combined utilization of the stable and radioactive isotopes is thus more interesting and robust to explore the movement processes of soil water in the thick vadose zones.

The objectives of this study are to explore the recharge mechanism of deep soil water and the corresponding impacts of deep-rooted fruit trees. The potential novelties of this study may include two aspects: (i) the stable and radioactive isotopes in water were combined to interpret the recharge mechanism of deep soil water, and (ii) the multiple components of SWB were partitioned to interpret the land use change effects. In specific, the radioactive isotopes were used to identify soil water recharge mechanisms and quantify deep drainage, while the stable isotopes were employed to determine source water and partition evapotranspiration. The results are important for understanding the water cycle, sustainable management of agriculture, and subsurface water resources in arid regions.

2. Materials and methods

2.1. Study area

Our study area is situated at the Daning County (110°27′−111°01′ E and 36°16′−36°36′ N), Shanxi Province of China (Fig. 1a). The annual average precipitation is 528 mm with 53% of them falling between July and September (Li et al., 2017a), and the mean annual temperature is 10.4 °C (1957−2017). The study area is relatively flat without runoff, and the soil is comprised of predominant silt loam. The soil bulk density is 1.25 g cm^{-3}. The water table ranges from 40 to 60 m below the surface. The land use patterns mainly include farmlands and economic orchards. With typical rain-fed agriculture, there is no irrigation in this region.

2.2. Sampling and analyzing

Four deep soil cores were collected under different land use types in August 2018 (Fig. 1b): one is farmland (F), which is cultivated with maize; the remaining are orchards, which are 8-year-old apple (A8), 12-year-old peach (P12), and 25-year-old apple (A25), respectively. The orchards were all converted from croplands. The distance among the four sites was close enough to share similar climate, soil and hydrogeology. In consequence, the differences in soil water profiles reflect the impact of plants to the greatest extent. This assumption has been validated by our previous study in which the soil water profiles at five sites under the same land use type were similar (Huang et al., 2018). As such, it is not necessary to conduct replicated sampling for each land use type, which will be further discussed later.

At each site, soil samples were obtained using a hollow-stem auger at an interval of 20 cm. The boreholes were drilled to 15 and 20 m deep. We divided each soil sample into two subsamples. One subsample was stored in an aluminum box to measure water contents by oven drying method at 105 °C for 8 h, and the other subsample was refrigerated at 4 °C in a sealed plastic bottle. Soil water storage was calculated by multiplying water content with bulk density. Soil water was collected by cryogenic vacuum extraction (Li et al., 2019b; Orlowski et al., 2016). In specific, soil samples were heated at 100 °C for two hours to evaporate water, and then evaporation water was trapped by a freezing system. The magnetic susceptibility was measured by a Bartington MS2 system with air-dried soil of ~10 g.

Precipitation samples were collected for each wet event from an open field near A25 (Fig. 1b), between September 2018 and November 2019. The stable oxygen and hydrogen isotopes in 107 soil water samples and 37 precipitation samples were measured by isotopic liquid water analyzer (LGR LIWA V2, USA) with a precision of 0.5‰ for $\delta^{2}H$ and 0.1‰ for $\delta^{18}O$. The water samples were measured against three standards covering the isotopic ranges of the study area (LGR3C: $\delta^{2}H$=−97.3‰, $\delta^{18}O$=−13.4‰; LGR4C: $\delta^{2}H$=−51.6‰, $\delta^{18}O$=−7.9‰; and LGR5C: $\delta^{2}H$=−9.2‰, $\delta^{18}O$=−2.7‰), and then analyzed by the LGR's Post-Analysis Software package including injected volume correction, linear fitting of calibration standards, and internal control monitoring. Isotope ratios are expressed in per mil (‰) relative to Vienna Standard Mean Ocean Water (VSMOW). In addition, the extracted water samples (n = 19) from soil profiles under the farmland were used to measure tritium by a liquid scintillation counter (Quantulus 1220, Perkin Elmer) with 2.0 TU as the detection limit.

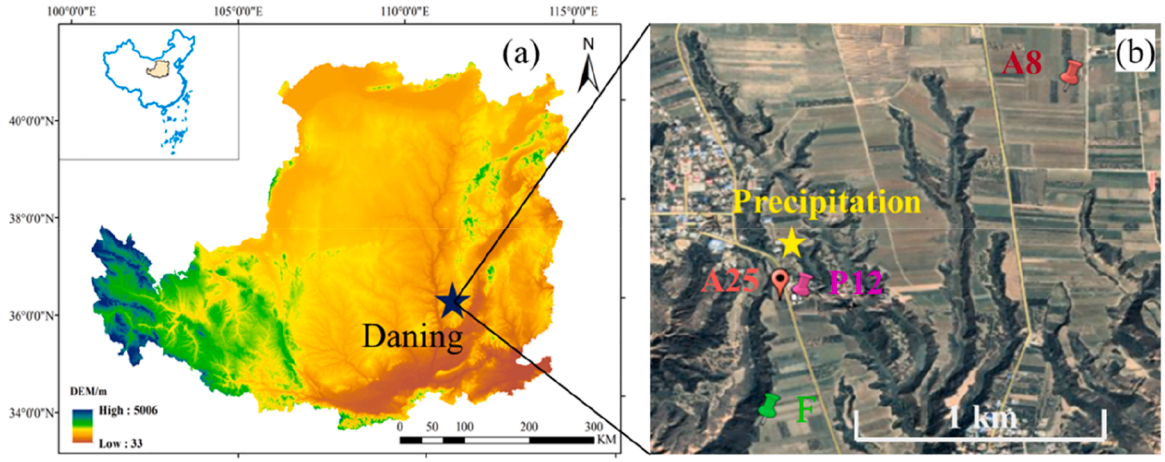

Fig. 1. The geographic location of the study area (a), the precipitation and soil sampling sites (b).

2.3. Identifying source water of soil

As the sampling sites in this study only receive water from precipitation, the purpose of this section is to determine the types of precipitation recharging soil at different depths. It can be conducted by connecting soil water isotopes with precipitation isotopes. If soil water stable isotopes fall below the Local Meteoric Water Line (LMWL), it is often interpreted as the isotope fractionation effect of precipitation due to evaporation (Allison and Hughes, 1983; Sprenger et al., 2017). To obtain the original isotopes of source water, we shifted soil water isotope values back to the LMWL along the soil water evaporation line (SW-EL) (Allen et al., 2019; Benettin et al., 2018). As the traditional regression approach for SW-EL estimation may yield biased estimates of source water isotopes (Benettin et al., 2018; Bowen et al., 2018), we calculated the EL slope using Eq. (1) based on the Craig-Gordon model (Benettin, 2018; Gibson et al., 2008).

$$Slope_{EL} = \frac{\left[\left(1-h+\varepsilon_k 10^{-3}\right)\right]_O \left[h\left(\delta_p-\delta_A\right)-\varepsilon\left(1+10^{-3}\delta_p\right)\right]_H}{\left[\left(1-h+\varepsilon_k 10^{-3}\right)\right]_H \left[h\left(\delta_p-\delta_A\right)-\varepsilon\left(1+10^{-3}\delta_p\right)\right]_O} \quad (1)$$

where h is relative humidity [–], and δ_A is the isotopic composition of atmospheric vapor [‰] estimated as $\delta_A = (\delta_P - \varepsilon^+)/\alpha^+$ (Benettin et al., 2018; Gibson and Reid, 2014). δ_P is the monthly amount-weighted precipitation isotopes, and ε is the total fractionation factor [‰] equal to the sum of equilibrium fractionation factor (ε^+) [‰] and kinetic fractionation factor (ε_k) [‰]. ε^+ and $\alpha^+$are the temperature-dependent equilibrium fractionation factors (Horita and Wesolowski, 1994), $\varepsilon^+ = (\alpha^+ - 1) \times 1000$. ε_k is calculated according to Benettin et al. (2018).

$$10^3 \ln\left[\alpha^+\left({}^2\mathrm{H}\right)\right] = \frac{1158.8T^3}{10^9} - \frac{1620.1T^2}{10^6} + \frac{794.84\mathrm{T}}{10^3} - 161.04 + \frac{2.9992\times10^9}{T^3} \quad (2)$$

$$10^3 \ln\left[\alpha^+\left({}^{18}O\right)\right] = -7.685 + 6.7123\frac{10^3}{T} - 1.6664\frac{10^6}{T^2} + 0.3504\frac{10^9}{T^3} \quad (3)$$

$$\varepsilon_k\left({}^2H\right) = n(1-h)(1-0.9755) \quad (4)$$

$$\varepsilon_k\left({}^{18}O\right) = n(1-h)(1-0.9723) \quad (5)$$

where the parameter n represents aerodynamic diffusion, and it ranges between 0.5 (saturated soil conditions) and 1 (very dry soil conditions). n was set as 0.75 because the evaporating soil layer has alternative saturating and drying conditions over time in this study.

To consider the seasonal variations of evaporation fractionation, the equilibrium (Horita and Wesolowski, 1994) and kinetic fractionation factors (Gat, 1996) for evaporation were estimated using the long-term (1957–2017) climatic variables (monthly mean temperatures and relative humidity). Further, we estimated the EL combing these fractionated factors with the corresponding monthly-amount weighted precipitation isotopes. The calculated EL slope ranged from 2.8 to 3.7 with an average of 3.1, which was further used to calculate the isotopic values of the original soil water sources by a Bayesian-type statistical approach (Bowen et al., 2018).

The daily precipitation stable isotopes were aggregated into monthly-based isotope data. To extend the data length, these data were combined with those from Xi'an and Taiyuan in the IAEA Global Network of Isotopes in Precipitation (IAEA/WMO, 2019). Based on monthly oxygen and hydrogen isotopes data ($n = 140$), the LMWL was determined as δ^2H=7.33 δ^{18}O + 4.48 ($R^2 = 0.92$, $P < 0.01$) by least square regression method.

2.4. Effects of vegetation on soil water recharge

Under farmland, the soil water can be consumed and replenished easily since the shallow-rooted plants consume much less water than deep-rooted plants. In consequence, farmland maintains a long-term SWB, and it is thus reasonable to take farmland as a reference to evaluate the impacts of deep-rooted fruit trees (Yang et al., 2012). To investigate the land use change effects on DSW recharge, we will directly compare the water storage and recharge rates estimated for different land uses. Further, to interpret the mechanism behind the changes, we will decompose each component of SWB (Eq. (6)).

$$\Delta S + D = P - E - T - R \quad (6)$$

where P is precipitation, E represents soil evaporation, T is transpiration, D represents deep drainage, ΔS is the change of soil water storage. R is surface runoff, which can be ignored because the study area is relatively flat with negligible runoff. The unit of each component is mm yr^{-1}.

2.4.1. Soil water deficit and deep drainage

ΔS can be estimated as soil water deficit between farmland and orchard, which is the differences in soil water storage between farmland and orchard divided by the stand age of fruit trees. D under farmland was estimated using the tritium peak method with the assumption that soil water moves in the form of piston flow (Allison et al., 1990), but the values under deep-rooted fruit trees can be estimated by incorporating ΔS (Eq. (8)) (Zhang et al., 2018).

$$D_{sr} = \theta \frac{Z_f - Z_a}{\Delta t} \quad (7)$$

$$D_{dr} = D_{sr} - \Delta S \quad (8)$$

where D_{sr} and D_{dr} is the deep drainage under farmland and orchards, respectively, mm yr^{-1}. θ is mean volumetric water content of the entire soil profile, cm^3 cm^{-3}. Z_f and Z_a are respectively tritium peak depth and active rooting zone depth, cm. The depth of 2 m was used for Z_a according to observation of soil water content (Li et al., 2019a). Δt is the elapsed years of the 1963-tritium peak, year.

2.4.2. Soil evaporation

To investigate the effects of vegetation types on soil evaporation, we first employed line-conditioned excess (lc-excess) to qualitatively compare the evaporation conditions under different land uses (Landwehr and Coplen, 2006).

$$lc-excess = \delta^2 H - a\ \delta^{18} O - b \quad (9)$$

where a and b represent the slope and intercept of LMWL, respectively. The lc-excess in precipitation is defined as zero. The negative lc-excess values suggest isotopic evaporative enrichment of water, and smaller lc-excess values suggest stronger evaporation (Sprenger et al., 2017).

Further, we employed the steady-state isotope mass balance model (Eq. (10)) to calculate the fractions of evaporation loss to the input water evaporating before being used by plants. This model considers that the input water is balanced by fractionated (evaporation) and non-fractionated (transpiration and deep seepage) water. It was derived from the approaches for evapotranspiration partitioning (Gibson and Edwards, 2002; Good et al., 2014; Yepez et al., 2003), and has been reframed for estimation of evaporation losses (Al-Oqaili et al., 2020). Assuming that the input water originates from local precipitation, E can be calculated through multiplying the evaporation loss fraction by precipitation. We estimated the average value of E/I ratios (%) with δ^2H and δ^{18}O.

$$E\Big/I = \frac{\delta_I - \delta_S}{\delta_E - \delta_S} \quad (10)$$

where δ_I is the original isotopes of input water calculated according to Bowen (2018) [‰], and δ_S is defined as the soil water isotopes under investigation [‰], δ_E is the isotopic composition of evaporated water [‰], which can be calculated by Eq. (11) based on Craig-Gordon model (1965).

$$\delta_E = \frac{(\delta_S - \varepsilon^+)/\alpha^+ - h\delta_A - \varepsilon_k}{1 - h + \varepsilon_k/1000} \quad (11)$$

2.4.3. Transpiration

The changes in transpiration can be easily estimated since each component of the water balance in Eq. (6) was quantified except for *T*. *T* can be used to evaluate the effects of root water uptake.

2.5. Statistical analysis

We tested the differences in soil water isotopes (δ^2H, δ^{18}O) between sampling sites, or depths by the *t*-test ($p = 0.05$). The differences in soil water contents and stable isotopes among different land uses were tested by the one way analysis of variance (ANOVA).

3. Results

3.1. Stable isotopes in precipitation

The daily δ^{18}O values in precipitation ranged between −18.3 and −2.0‰ with a mean value of −9.2 ± 3.4‰ (mean ± SD), while the δ^2H ranged between −131.4 and −2.4‰, with a mean value of −62.2 ± 27.8‰. The monthly volume-weighted isotope values of precipitation have similar but smaller ranges of isotopes compared with daily values (Fig. 2). Overall, either on daily or monthly scale, the precipitation isotopes had large seasonal variations. In specific, the months with larger precipitation amounts (e.g. July to September in rainy season) had more depleted isotopic compositions than the other months, especially those in dry season (Fig. 2). The seasonality and amount effect of precipitation isotopes suggested that precipitation of different intensities may be used to link with soil water to discuss the potential recharge.

3.2. Soil profiles

The soil water contents in the shallow soils (0–4 m) varied greatly with depth and land use types, while it relatively stabilized below 4 m relative to shallow soils (Fig. 3a). There is an obvious abrupt peak at 13 m below the soil surface because of the paleosol with higher clay contents (Huang et al., 2019). With increasing stand ages of fruit trees, the soil water contents below 4 m decreased from 15.6% to 7.4%. In consequence, the soil water storage of the whole profiles was the lowest under A25 (1654.7 ± 4.7 mm) and the largest under farmland (2823.7 ± 5.3 mm) (Table 1), which suggests the impacts of deep-rooted fruit trees on soil water. The magnetic susceptibility was well correlated with soil conditions, and the depth with high values suggested the existence of paleosol with high clay and water contents (Huang et al., 2019). As such, the variations in water profiles were very similar as those of magnetic susceptibility, especially in the deep layers around 13 m (Fig. 3b). This phenomenon suggests the homogenous stratified structure of loess deposits, which confirmed that our sampling without replication can exclude the impacts of soil conditions and represent the impacts of land use types.

The soil water δ^{18}O varied with the soil depths within 0–6 m, but were relatively stable below 6 m of the surface (Fig. 3c). Under four land use types, the δ^{18}O or δ^2H values for 0–6 m soils were significantly different ($p < 0.05$), ranging from −8.7 ‰ to −9.6‰ and −73.2‰ to −79.2‰, while those below 6 m are less variable (−9.5‰ to −9.8‰ for δ^{18}O, and −79.8‰ to −82.8‰ for δ^2H) (One-Way ANOVA, $p > 0.05$). Besides, the isotopic signals were more enriched in shallow soils than that of deep soils (T-test, $p < 0.05$). It implies that the depth of 6 m can be used as the critical depth subject to evaporation. Further, the lc-excess values were highly variable in soil profiles above 6 m ($p < 0.05$), but stable within 6–10 m under the four land uses (Fig. 3d and Table 1), which further confirmed the deduction about critical depth of evaporation. However, the averaged lc-excess values in the soil profiles above 6 m were more positive than those below 6 m, suggesting that soil water above 6 m has less evaporation. The tritium profile under farmland had a clear tritium peak of 74.9 TU at the depth of ~8 m (Fig. 3e). Further, the tritium profile appears to be a parabolic curve, suggesting the occurrence of piston flow; therefore, the tritium peak depth suggested the moving distance of the 1963-precipitation.

To investigate the land use change effects on SWB, it is crucial to determine a critical depth to cover the periods occurring land use

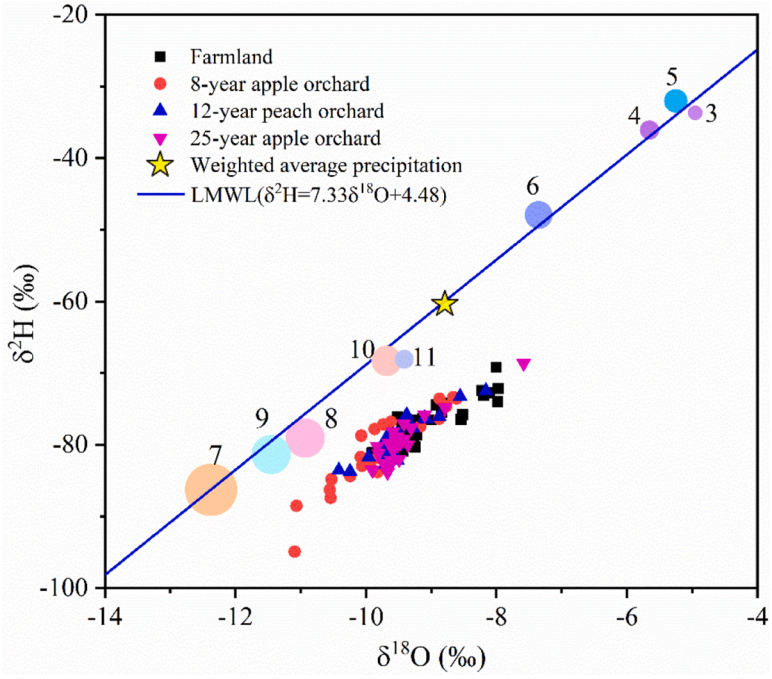

Fig. 2. Dual isotopes plot of precipitation and soil water. Numbers in the figure represent the month of each year, and circle size denotes the monthly mean precipitation amount.

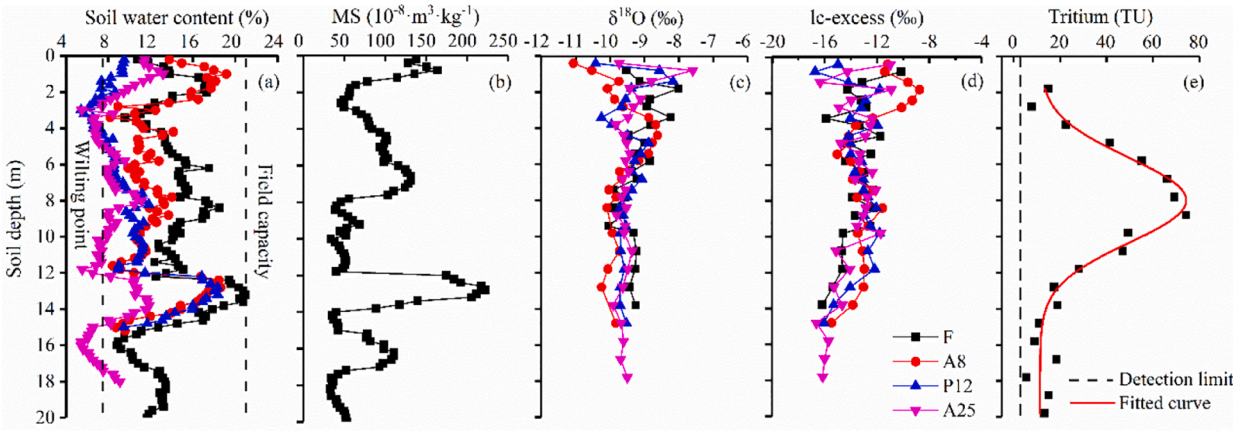

Fig. 3. Soil profiles of water content (a), magnetic susceptibility (b), oxygen isotopes (c), lc-excess values (d), and tritium (e). Subplots (a), (c), and (d) share the same legend presented in (d): F, A8, P12, and A25 represent farmland, 8-year apple orchard, 12-year peach orchard, and 25-year apple orchard, respectively.

Table 1
Water storage, stable isotopes and lc-excess of soil profiles for the four land uses.

Land use	SWS (mm)		δ^{18}O (‰)		δ^{2}H (‰)		lc-excess (‰)	
Types	0–15	6–15	0–6	6–20	0–6	6–20	0–6	6–20
F	2823.7(5.2)	1802.9(6.2)	−8.7(0.5)	−9.5(0.3)	−73.3(2.9)	−79.8(1.3)	−13.8(1.3)	−14.1(1.4)
A8	2430.4(7.2)	1413.4(6.9)	−9.5(0.7)	−9.8(0.4)	−79.2(4.3)	−82.2(4.1)	−12.4(2.5)	−13.9(1.3)
P12	1943.2(3.4)	1359.8(7.6)	−9.4(0.6)	−9.6(0.1)	−76.3(3.5)	−80.7(1.9)	−13.6(1.4)	−13.6(1.4)
A25	1653.7(4.7)	988.4(4.1)	−9.8(0.5)	−9.6(0.1)	−83.6(3.3)	−79.6(1.5)	−13.5(1.0)	−14.4(1.2)

Note: SWS: soil water storage; Number in bracket is the standard error.

change. As the depth of 8 m has water of ~55 years old, the infiltration rates can be estimated by an equation similar as Eq. (7), i.e. infiltration rates = $(Z_f - Z_a)/\Delta t$ =(8 m −2 m)/55 years=10.9 cm year^{-1}. The fruit trees are no older than 30 years, the depth covering the period of land use change can thus be estimated as (Z_a+10.9 cm year^{-1} × 30 years) = 5.3 m. Considering that the depth profile of 0–6 m is also subject to evaporation according to the isotope profiles, it is reasonable to use 6 m as the critical depth. In consequence, the land use change effects can be investigated by focusing on different SWB components in different layers. For example, the land use change effects on evaporation loss can be investigated with the shallow layers, i.e. 0–6 m.

3.3. Soil water sources

Soil water isotopes fell below LMWL (Fig. 2), suggesting that soil water may originate from the local precipitation but has experienced evaporation effects. This is true for this area since the water tables are below 40 m and the sampled soils cannot be recharged by upward capillary water. We further identified the isotope values of the original sources for soil water by shifting SW-EL back to the LMWL. Grouped by depth profiles, the recharging source for shallow and deep soil waters had δ^{18}O and δ^{2}H of (−12.6‰, −87.8‰), and (−13.0‰, −90.8‰), respectively (Fig. 4a). The δ^{18}O and δ^{2}H of source waters were not significantly different for the shallow and deep layers ($p > 0.05$), but

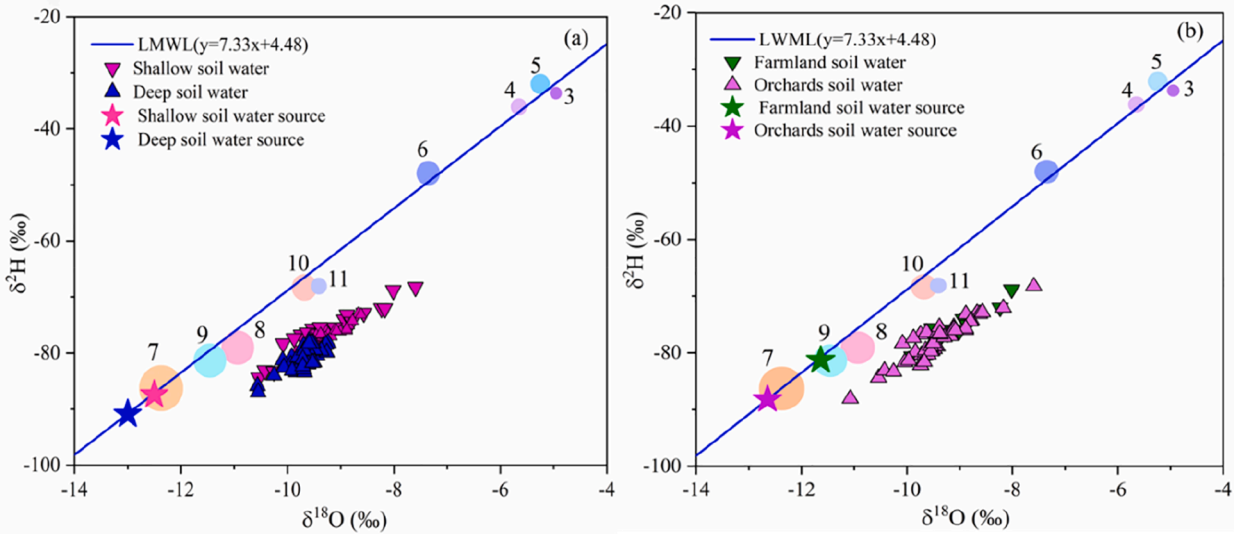

Fig. 4. δ^{18}O versus δ^{2}H of monthly precipitation, calculated source water isotopic signatures presented according to respective soil layers (a) and land use types (b). Numbers in figure represent the month of each year, and circle size denotes the monthly average precipitation amount.

both close to those of precipitation in rainy season, i.e. July to September. Theoretically, the deep soils need source water with more depleted isotopes than the shallow soils since they need more intensive precipitation. As such, it is reasonable for deep soils to have source water isotopically similar as the rainy-season precipitation. However, this is also the case for shallow soils though they are assumed to have more isotopically enriched water close to the annual volume-weighted values. The reason for this is probably because the samples were collected in rainy season, which may be subject to intensive rainfall input with more depleted isotopic signals prior to soil sampling.

However, in the shallow layers, the source water under orchards (−12.8‰, −89.3‰) was more isotopically depleted than that of farmland (−11.6‰, −81.2‰) ($p < 0.05$) (Fig. 4b), indicating that soil water under orchards required extreme rainfall with more depleted isotope signals as recharge source, or subject to less evaporative enrichment. Nevertheless, in deep layers, the source water under farmland and orchard was similar with $\delta^{18}O$ and $\delta^{2}H$ of −13.2‰ and −92.3‰, respectively. The insignificant difference in source water of deep soils under different land use types may reflect the pure impacts of precipitation since those depth profiles reflect the period with the same land use as farmland.

3.4. Soil water balance components

Relative to farmland, the soil water deficit under A8, P12 and A25 was 49.2, 73.4, and 46.8 mm yr^{-1}, respectively (Table 2). The estimated deep drainage under farmland was 25.8 mm yr^{-1}, accounting for 5% of the mean annual precipitation. However, deep drainage under the deep-rooted fruit trees would be zeros because of the water deficit. The mean annual ET was 502.2 mm under farmland, accounting for 95% of the annual average precipitation. According to the water balance equation, the mean annual ET was respectively 577.2, 601.4, and 574.8 mm under A8, P12 and A25, and contributed to 109−114% of the mean annual precipitation. Further partition of ET showed that the annual average E was 205.9, 195.4, 184.8, and 179.5 mm, while the mean annual T was 296.3, 381.8, 416.6, and 395.3 mm for F, A8, P12 and A25, respectively; consequently, the mean annual E and T accounted for 31%−41% and 59−69% of the total ET, respectively. The mean annual T/ET appeared to increase with increasing ages of fruit trees since the values were 59%, 66%, 69% and 69% under F, A8, P12 and A25, respectively.

4. Discussion

4.1. Origin and recharge possibility of deep soil water

Water in deep soils greatly contributes to seasonal drought relief (Fang et al., 2016; Giardina et al., 2018; Zunzunegui et al., 2017); however, the recharge possibility and mechanism have not been fully investigated in semi-arid and arid regions with intensive root water uptake. Here, water stable and radioactive isotopes were combined to identify the recharge source and mechanism of DSW (> 6 m) under fruit orchards in the Loess Plateau. First, the similarity in tritium profile with historical precipitation tritium time series implied that soil water is likely to come from precipitation in the form of piston flow (Cook et al., 1994; Li et al., 2019c), and the dual-isotope comparison further showed that soil water may originate from precipitation but has experienced strong evaporation (Evaristo et al., 2015; Sprenger et al., 2017). Second, the identified source water of soils > 6 m indicated that DSW may only originate from the flood season, i.e. July to September (Fig. 4), with intensive rainfall events (Jasechko and Taylor, 2015; Zimmermann et al., 1966). Our results may be supported by Liu et al. (2010), who reported that the extreme high precipitation in 2003 (954 mm, 63.4% higher than the long-term average) can recharge soil to a depth of 6 m at Changwu loess tableland though the temporal variability of soil water rarely exceeds 2 m. By extension, the water stable isotopes in soil layers > 6 m may represent those of the recharged water under farmlands 30 years ago.

The soil profiles of water content and isotopes indicated the occurrence of piston flow under each sampling site, which had been observed in other sites on the Loess Plateau (Li et al., 2018a; Lin and Wei, 2006; Zhang et al., 2017). In consequence, the DSW is difficult to be recharged in this region associating with low infiltration velocity and limited rainfall (Huang et al., 2019). Even for tropic ecoregions, the soil water can only be replenished to the depth of 8 m in the wettest sites (annual rainfall > 1000 mm), while most sites are unlikely to be fully replenished in the next growing season (Mendham et al., 2011). As a result, DSW is hardly to be replenished in normal precipitation years in most regions, and it is even more difficult for the dry regions with limited rainfall but thick soils.

4.2. Impacts of deep-rooted fruit trees on soil water recharge

This study indicated that the conversion from farmland to deep-rooted fruit trees decreased soil water storage, which is consistent with other studies indicating the effect of afforestation on soil drying (Farley et al., 2005; Jia et al., 2017; Schwarzel et al., 2019). In particular, the reduced water storage in deep soils appeared to increase with stand age of fruit trees (Table 1), which highlighted the strong root water uptake of fruit trees (Jia et al., 2017; Li et al., 2018b; Nepstad et al., 1994). However, the estimated soil water deficit under orchards was larger than the deep drainage under farmland, implying the deep-rooted fruit trees terminated the recharge of DSW (Li et al., 2019a, 2018a).

The large soil water deficit and reduced deep drainage under orchards can be attributed to substantial water consumption by ET (Condon et al., 2020; Maxwell and Condon, 2016). The estimated ratio of ET to annual average precipitation under farmland was 95%, but the values for fruit orchards were 109−114% (Table 2). Further partition of ET showed that the conversion from farmland to orchards decreased soil evaporation loss but increased transpiration (Table 2). As such, the soil water deficit is likely to be dominated by increasing transpiration from root water uptake. As such, the mechanism behind the changes in soil water can be interpreted by the connection between soil water and plant growth. In specific, with increasing ages, the root system of fruit trees is getting more developed and deepening to mine more old water to maintain growth (Li et al., 2018b). Chronically, the depletion of soil water can be detected in deep layers and further terminate deep drainage (Fig. 3a and Table 2).

4.3. Uncertainties and implications

This study decomposed each component of SWB by combining stable and radioactive water isotopes. To validate our methods, we compared the results with those from local or global scale studies. As water storage and deep drainage in soils were directly estimated from the observation, the indirectly estimated ET (the residual of precipitation, soil water storage, and deep drainage) should be reliable. Further comparison showed that the estimated values overlapped with previous studies in the Loess Plateau and across the globe. For example, the ratio of ET to precipitation was 95–114% (Table 2), which was similar as the values of

Table 2
The estimated components of soil water balance under different land use types.

Land use types	ΔS (mm yr^{-1})	D (mm yr^{-1})	ET (mm yr^{-1})	E (mm yr^{-1})	T (mm yr^{-1})	ET/P %
F	-	25.8	502.2	205.9	296.3	95
A8	49.2	0	577.2	195.4	381.8	109
P12	73.4	0	601.4	184.8	416.6	114
A25	46.8	0	574.8	179.5	395.3	109

Note: ΔS: soil water deficit; D: deep drainage; ET: evapotranspiration; E: evaporation; T: transpiration, P: annual average precipitation.

94−110% from different methods in the Loess Plateau (Li et al., 2019a; Wang and Wang, 2017; Wang et al., 2016). The estimated E/ET was 31−41% in this study, similar as those from 52 studies across the globe (20−40%) (Kool et al., 2014). The T/ET was 59−69% in this study, which agreed with recent globally derived estimates (60−80%) (Good et al., 2015; Jasechko et al., 2013; Schlesingera and Jasechko, 2014). The employed methods presented reliable results for SWB and provide an alternative method for related studies.

Soil water is crucial for agricultural production and groundwater recharge, but the substantial land use changes from farmland to forestland would significantly alter the water balance (Gates et al., 2011; Schwarzel et al., 2019). In this study, the deep-rooted fruit trees excessively consumed deep old soil water by transpiration. The large soil water reservoir stored in the loess deposits to 350 m deep plays a vital role and even governs the hydrological processes (Li et al., 2019b, 2017b). As large-scale afforestation has been implemented in the Loess Plateau (Chen et al., 2019; Du et al., 2020; Schwarzel et al., 2019), the effects of afforestation on soil drying detected in this study have been reported elsewhere (Wang et al., 2011). It is thus urgent to investigate the sustainability of vegetation and water resources.

Despite that tree-planting is popular for climate change, land degradation, and biodiversity loss (e.g. Great Green Wall initiative in Africa, Restoration Initiative in Asia, and Grain for Green Program in China) (Bastin et al., 2019; Chen et al., 2015), the trade-off between evapotranspiration and recharge of DSW has been poorly understood. This study is a pioneering attempt to quantify the effects of deep-rooted fruit trees on SWB combining water stable and radioactive isotopes. Our work provides insights for regions with large-scale afforestation to avoid threats on water security, which is especially important for the arid and semiarid regions. Further, global warming has resulted in more extreme climate events, which may have great impacts on plant growth and SWB (Erler et al., 2019; Scheiter et al., 2020). As such, the detected effects of afforestation on DSW recharge should be further evaluated for adaptation of climate change.

5. Conclusion

This study combined water stable and radioactive isotopes to investigate the recharge source of DSW and characterized the impacts of land use change on SWB. We found that the soil water below 6 m mainly originated from intensive rainfall events in wet season (July and September), which had an age over 55 years old. The conversion from farmland to deep-rooted fruit trees significantly reduced soil evaporation loss, but increased transpiration by root water uptake, and further terminated DSW recharge. This study provides information for land management and water regulation in regions with large-scale tree-planting, especially for dry regions.

Declaration of Competing Interest

The authors have no conflict of interest to declare.

Acknowledgements

This study was jointly funded by the National Natural Science Foundation of China (42071043), Natural Science Foundation of Shaanxi Province (2018JZ4001) and the Talent Program of Northwest A&F University (2452020002). We appreciate the technical help from Jingjing Jin, Institute of Water-saving Agriculture in Arid Areas of China, Northwest A&F University.

References

Al-Oqaili, F., Good, S.P., Peters, R.T., Finkenbiner, C., Sarwar, A., 2020. Using stable water isotopes to assess the influence of irrigation structural configurations on evaporation losses in semiarid agricultural systems. Agric. For. Meteorol. 291, 108083.

Allen, S.T., Kirchner, J.W., Braun, S., Siegwolf, R.T.W., Goldsmith, G.R., 2019. Seasonal origins of soil water used by trees. Hydrogeol. Earth Syst. Sci. 2 (23), 1199–1210.

Allison, G.B., et al., 1990. Land clearance and river salinisation in the western Murray Basin, Australia. J. Hydrol. 119 (1), 1–20.

Allison, G.B., Hughes, M.W., 1983. The use of natural tracers as indicators of soil-water movement in a temperate semi-arid region. J. Hydrol. 60 (1), 157–173.

Bastin, J.-F., et al., 2019. The global tree restoration potential. Science 365 (6448), 76–79.

Benettin, P., et al., 2018. Effects of climatic seasonality on the isotopic composition of evaporating soil waters. Hydrol. Earth Syst. Sci. 22 (5), 2881–2890.

Blöschl, G., et al., 2019. Twenty-three unsolved problems in hydrology (UPH) – a community perspective. Hydrol. Sci. J. 64 (10), 1141–1158.

Bowen, G.J., et al., 2018. Inferring the source of evaporated waters using stable H and O isotopes. Oecologia 187 (4), 1025–1039.

Brooks, J.R., Barnard, H.R., Coulombe, R., McDonnell, J.J., 2009. Ecohydrologic separation of water between trees and streams in a Mediterranean climate. Nat. Geosci. 3 (2), 100–104.

Bryan, B.A., et al., 2018. China's response to a national land-system sustainability emergency. Nature 559 (7713), 193–204.

Cao, R., et al., 2018. Deep soil water storage varies with vegetation type and rainfall amount in the Loess Plateau of China. Sci. Rep. 8 (1), 12346.

Carrière, S.D., et al., 2020. The role of deep vadose zone water in tree transpiration during drought periods in karst settings – Insights from isotopic tracing and leaf water potential. Sci. Total Environ. 699, 134332.

Chen, C., et al., 2019. China and India lead in greening of the world through land-use management. Nat. Sustain. 2, 122–129.

Chen, L., Huang, Z., Gong, J., Fu, B., Huang, Y., 2007. The effect of land cover/vegetation on soil water dynamic in the hilly area of the loess plateau, China. Catena 70 (2), 200–208.

Chen, Y., et al., 2015. Balancing green and grain trade. Nat. Geosci. 8 (10), 739–741.

Condon, L.E., Atchley, A.L., Maxwell, R.M., 2020. Evapotranspiration depletes groundwater under warming over the contiguous United States. Nat. Commun. 11 (1), 873.

Cook, P.G., et al., 1994. Unsaturated zone tritium and chlorine 36 profiles from southern Australia: their use as tracers of soil water movement. Water Resour. Res. 30 (6), 1709–1719.

Craig, H. and Gordon, L.I., 1965. Deuterium and oxygen 18 variations in the ocean and marine atmosphere. In: E. Tongiogi (Editor), Stable Isotopes in Oceanographic Studies and Paleotemperatures. Pisa, Spoleto, Italy, pp. 9–130.

Deng, Y., et al., 2020. Vegetation greening intensified soil drying in some semi-arid and arid areas of the world. Agric. For. Meteorol. 292-293, 108103.

Du, X., et al., 2020. Quantitatively assessing and attributing land use and land cover changes on China's Loess Plateau. Remote Sens. 12 (353), 1–18.

Erler, A.R., et al., 2019. Evaluating climate change impacts on soil moisture and groundwater resources within a lake-affected region. Water Resour. Res. 55 (10), 8142–8163.

Evaristo, J., Jasechko, S., McDonnell, J.J., 2015. Global separation of plant transpiration from groundwater and streamflow. Nature 525 (7567), 91–94.

Evaristo, J., et al., 2019. Characterizing the fluxes and age distribution of soil water, plant water, and deep percolation in a model tropical ecosystem. Water Resour. Res. 55 (4), 3307–3327.

Fang, X., et al., 2016. Variations of deep soil moisture under different vegetation types and influencing factors in a watershed of the Loess Plateau, China. Hydrol. Earth Syst. Sci. 20 (8), 3309–3323.

Farley, K.A., Jobbagy, E.G., Jackson, R.B., 2005. Effects of afforestation on water yield: a global synthesis with implications for policy. Glob. Chang. Biol. 11 (10), 1565–1576.

Gat, J.R., 1996. Oxygen and hydrogen isotopes in the hydrologic cycle. Annu. Rev. Earth Planet. Sci 24, 225–262.

Gates, J.B., Scanlon, B.R., Mu, X.M., Zhang, L., 2011. Impacts of soil conservation on groundwater recharge in the semi-arid Loess Plateau, China. Hydrogeol. J. 19 (4), 865–875.

Geris, J., Tetzlaff, D., McDonnell, J., Soulsby, C., 2015. The relative role of soil type and tree cover on water storage and transmission in northern headwater catchments. Hydrol. Process 29 (7), 1844–1860.

Giardina, F., et al., 2018. Tall Amazonian forests are less sensitive to precipitation variability. Nat. Geosci. 11 (6), 405–409.

Gibson, J.J., Birks, S.J., Edwards, T.W.D., 2008. Global prediction ofδAandδ2H-δ18O evaporation slopes for lakes and soil water accounting for seasonality. Glob. Biogeochem. Cycl. 22 (2) n/a-n/a.

Gibson, J.J., Edwards, T.W.D., 2002. Regional water balance trends and evaporation-transpiration partitioning from a stable isotope survey of lakes in northern Canada. Glob. Biogeochem. Cycl. 16 (2), 10-1-10-14.

Gibson, J.J., Reid, R., 2014. Water balance along a chain of tundra lakes: a 20-year isotopic perspective. J. Hydrol. 519, 2148–2164.

Good, S.P., Noone, D., Bowen, G., 2015. Hydrologic connectivity constrains partitioning of global terrestrial water fluxes. Science 349 (624), 175–177.

Good, S.P., et al., 2014. d2H isotopic flux partitioning of evapotranspiration over a grass field following a water pulse and subsequent dry down. Water Resour. Res. 50 (1410–1432).

Horita, J., Wesolowski, D.J., 1994. Liquid-vapor fractionation of oxygen and hydrogen isotopes of water from the freezing to the critical temperature. Geochim. Cosmochim. Acta 58 (16), 3425–3437.

Huang, L., Shao, M.a., 2019. Advances and perspectives on soil water research in China's Loess Plateau. Earth-Sci. Rev., 102962

Huang, T., et al., 2019. How does precipitation recharge groundwater in loess aquifers? Evidence from multiple environmental tracers. J. Hydrol. 583, 124532.

Huang, Y., Chang, Q., Li, Z., 2018. Land use change impacts on the amount and quality of recharge water in the loess tablelands of China. Sci. Total Environ. 628–629, 443–452.
IAEA/WMO, 2019. Global network of isotopes in precipitation. The GNIP Datab. Accessible at: https://nucleus.iaea.org/wiser.
Jasechko, S., et al., 2013. Terrestrial water fluxes dominated by transpiration. Nature 496, 347–350.
Jasechko, S., Taylor, R.G., 2015. Intensive rainfall recharges tropical groundwaters. Environ. Res. Lett. 10 (12), 124015.
Jia, X., et al., 2014. The tradeoff and synergy between ecosystem services in the Grain-for-Green areas in Northern Shaanxi, China. Ecolog. Indica. 43, 103–113.
Jia, X., Shao, M.a., Zhu, Y., Luo, Y., 2017. Soil moisture decline due to afforestation across the Loess Plateau, China. J. Hydrol. 546, 113–122.
Jian, S., Zhao, C., Fang, S., Yu, K., 2015. Effects of different vegetation restoration on soil water storage and water balance in the Chinese Loess Plateau. Agric. For. Meteorol. 206, 85–96.
Kendy, E., et al., 2003. A soil-water-balance approach to quantify groundwater recharge from irrigated cropland in the North China Plain. Hydrol. Process. 17 (10), 2011–2031.
Kool, D., et al., 2014. A review of approaches for evapotranspiration partitioning. Agric. For. Meteorol. 184, 56–70.
Landwehr, J.M., Coplen, T.B., 2006. Line-conditioned excess: a new method for characterizing stable hydrogen and oxygen isotope ratios in hydrologic systems. In: international Conference on Isotopes in Environmental Studies. IAEA, Vienna, pp. 132–135.
Li, B., Wang, Y., Hill, R.L., Li, Z., 2019a. Effects of apple orchards converted from farmlands on soil water balance in the deep loess deposits based on HYDRUS-1D model. Agric. Ecosyst. Environ. 285, 106645.
Li, H., Si, B., Li, M., 2018a. Rooting depth controls potential groundwater recharge on hillslopes. J. Hydrol. 564, 164–174.
Li, H., Si, B., Wu, P., McDonnell, J.J., 2018b. Water mining from the deep critical zone by apple trees growing on loess. Hydrol. Process. 33 (2), 320–327.
Li, J., Li, Z., Lü, Z., 2016. Analysis of spatiotemporal variations in land use on the Loess Plateau of China during 1986–2010. Environ. Earth Sci. 75 (11).
Li, Z., Chen, X., Liu, W., Si, B., 2017a. Determination of groundwater recharge mechanism in the deep loessial unsaturated zone by environmental tracers. Sci. Total Environ. 586, 827–835.
Li, Z., Coles, A.E., Xiao, J., 2019b. Groundwater and streamflow sources in China's Loess Plateau on catchment scale. Catena 181, 104075.
Li, Z., Jasechko, S., Si, B., 2019c. Uncertainties in tritium mass balance models for groundwater recharge estimation. J. Hydrol. 571, 150–158.
Li, Z., Lin, X., Xiang, W., Chen, X., Huang, T., 2017b. Stable isotope tracing of headwater sources in a river on China's Loess Plateau. Hydrolog. Sci. J. 62 (13), 2150–2159.
Li, Z., Zheng, F.-l., Liu, W.-z., Flanagan, D.C., 2010. Spatial distribution and temporal trends of extreme temperature and precipitation events on the Loess Plateau of China during 1961–2007. Quatern. Int. 226 (1–2), 92–100.
Lin, R., Wei, K., 2006. Tritium profiles of pore water in the Chinese loess unsaturated zone: implications for estimation of groundwater recharge. J. Hydrol. 328 (1–2), 192–199.
Maxwell, R.M., Condon, L.E., 2016. Connections between groundwater flow and transpiration partitioning. Science 353, 377–379.
Mendham, D.S., et al., 2011. Soil water depletion and replenishment during first- and early second-rotation Eucalyptus globulus plantations with deep soil profiles. Agric. For. Meteorol. 151 (12), 1568–1579.
Nepstad, D.C., et al., 1994. The role of deep roots in the hydrological and carbon cycles of Amazonian forests and pastures. Nature 372 (6507), 666–669.
Oki, T., Kana, S., 2006. Global hydrological cycles and world water resources. Science 313 (5790), 1068–1072.
Orlowski, N., Breuer, L., McDonnell, J.J., 2016. Critical issues with cryogenic extraction of soil water for stable isotope analysis. Ecohydrology 9 (1), 1–5.
Peng, S., Li, Z., 2018. Incorporation of potential natural vegetation into revegetation programmes for sustainable land management. Land Degrad. Develop. 29 (10), 3503–3511.
Peng, X., Guo, Z., Zhang, Y., Li, J., 2017. Simulation of long-term yield and soil water consumption in apple orchards on the Loess Plateau, China, in response to fertilization. Sci. Rep. 7 (1), 5444.
Scanlon, B.R., Tyler, S.W., Wierenga, P.J., 1997. Hydrologic issues in arid, unsaturated systems and implications for contaminant transport. Rev. Geophys. 35 (4), 461–490.
Scheiter, S., et al., 2020. Climate change promotes transitions to tall evergreen vegetation in tropical Asia. Glob. Chang. Biol.
Schlesingera, W.H., Jasechko, S., 2014. Transpiration in the global water cycle. Agric. For. Meteorol. 189-190 (6), 115–117.
Schwarzel, K., Zhang, L., Montanarella, L., Wang, Y., Sun, G., 2019. How afforestation affects the water cycle in drylands: a process-based comparative analysis. Glob. Chang. Biol. 00, 1–16.
Sprenger, M., et al., 2019. The demographics of water: a review of water ages in the critical zone. Rev. Geophys. 57.
Sprenger, M., Tetzlaff, D., Soulsby, C., 2017. Soil water stable isotopes reveal evaporation dynamics at the soil–plant–atmosphere interface of the critical zone. Hydrol. Earth Syst. Sci. 21 (7), 3839–3858.
Tang, Q., 2019. Global change hydrology: terrestrial water cycle and global change. Sci. China Earth Sci. 63 (3), 459–462.
Wang, C., Fu, B., Zhang, L., Xu, Z., 2018. Soil moisture–plant interactions: an ecohydrological review. J. Soils Sediments 19 (1), 1–9.
Wang, D., Wang, L., 2017. Dynamics of evapotranspiration partitioning for apple trees of different ages in a semiarid region of northwest China. Agricul. Water Manag. 191, 1–15.
Wang, Y., et al., 2020. Response of deep soil drought to precipitation, land use and topography across a semiarid watershed. Agric. For. Meteorol. 282-283, 107866.
Wang, Y., Shao, M.a., Zhu, Y., Liu, Z., 2011. Impacts of land use and plant characteristics on dried soil layers in different climatic regions on the Loess Plateau of China. Agric. For. Meteorol. 151 (4), 437–448.
Wang, Y., Wang, L., Han, X., Zhang, L., 2016. Evapotranspiration characteristics of apple orchard at peak period of fruiting in Loess Tableland. Scientia Silvae Sinicae 52 (01), 128–135.
Yang, L., Wei, W., Chen, L., Jia, F., Mo, B., 2012. Spatial variations of shallow and deep soil moisture in the semi-arid Loess Plateau, China. Hydrol. Earth Syst. Sci. 16 (9), 3199–3217.
Yepez, E.A., Williams, D.G., Scott, R.L., Lin, G., 2003. Partitioning overstory and understory evapotranspiration in a semiarid savanna woodland from the isotopic composition of water vapor. Agric. For. Meteorol. 119 (1–2), 53–68.
Zhang, Z., Li, M., Si, B., Feng, H., 2018. Deep rooted apple trees decrease groundwater recharge in the highland region of the Loess Plateau, China. Sci. Total Environ. 622-623, 584–593.
Zhang, Z.Q., Evaristo, J., Li, Z., Si, B.C., McDonnell, J.J., 2017. Tritium analysis shows apple trees may be transpiring water several decades old. Hydrol. Process. 31 (5), 1196–1201.
Zimmermann, U., Münnich, K.O., Roether, W., 1966. Tracers Determine Movement of Soil Moisture and Evapotranspiration. Science 152 (3720), 346–347.
Zunzunegui, M., et al., 2017. Reliance on deep soil water in the tree species Argania spinosa. Tree Physiol. 38 (5), 678–689.